Novel one-point calibration strategy for high-throughput quantitation of microcystins in freshwater using LC-MS/MS

Huiyan Zhang [a, b], Yanshen Li [c], Mohamed F. Abdallah [d, e], Haiguang Tan [a], Jianxun Li [a], Shuyan Liu [a], Rong Zhang [a], Feifei Sun [f], Yi Li [a,*], Shupeng Yang [a,*]

[a] Institute of Food Science and Technology, Chinese Academy of Agricultural Sciences, Beijing 100193, P. R. China.

[b] Institute of Animal Sciences, Chinese Academy of Agricultural Sciences, Beijing, 100193, P. R. China.

[c] College of Life Science, Yantai University, Yantai, Shandong, 264005, P. R. China.

[d] Department of Food Technology, Safety and Health, Ghent University, Coupure Links 653, 9000, Ghent, Belgium.

[e] Department of Forensic Medicine and Toxicology, Faculty of Veterinary Medicine, Assiut University, Assiut 71515, Egypt.

[f] College of Animal Science and Technology, Anhui Agricultural University, Hefei, 230036, P. R. China.

*Author to whom correspondence should be addressed:

Tel: +86-10-6281-3566; Fax: +86-10-6281-3566;

E-mail: yangshupeng@caas.cn (Shupeng Yang), and liyi01@caas.cn (Yi Li)

Abstract: Precise quantification of microcystins (MCs) in freshwater is crucial for environmental monitoring and human health. However, the preparation of traditional multi-sample external calibration curve (MSCC) is time consuming and prone to error. Here, a novel one-point calibration strategy including one sample multi-point calibration curve (OSCC) and in sample calibration curve (ISCC) is proposed for the quantitation of eight MCs in freshwater lakes using liquid chromatography tandem mass spectrometry (LC-MS/MS). The multiple isotopologue reaction monitoring (MIRM) of MCs and its ^{15}N-labeled internal standards were used for OSCC and ISCC, respectively. The isotopic abundance of each MIRM channel could be calculated and measured accurately. Additionally, this strategy was comprehensively validated and showed good performance in selectivity, sensitivity, accuracy and precision as the traditional MSCC. Interestingly, OSCC could realize sample dilution by monitoring the less abundant MIRM transitions, while ISCC remove blank matrixes and generate calibration curve in each study samples. Furthermore, the proposed methodology was successfully applied to analyze several freshwater lake samples contaminated by MCs. Considering the advantages of excluding the MSCC preparation, simplified workflows and improved throughput, OSCC and ISCC will be favored for MCs monitoring and as an emerging approach in environmental pollutant control and prevention.

Keyword: Microcystins, Calibration curve, Quantitative analysis, Isotopologue multipoint calibration, Water safety.

1. Introduction

Microcystins (MCs) are the most important cyanobacterial toxins produced during algae bloom, which are commonly found in lakes, rivers, and offshore of Mediterranean, Subtropical and Tropical Countries (Bouaicha et al., 2019; Janssen 2019; Kim et al., 2021). Several cyanobacterial genera including *Microcystis*, *Hapalosiphon* and *Anabaena* are known to produce MCs (Harke et al., 2016; Janssen 2019). MCs are primarily targeting the liver by inhibiting protein phosphatase types 1 and 2A, which leads to strong liver toxicity. The typical chemical structure of MCs is a cyclo-[D-Ala-L-X-D-erythrob-MeAsp-L-Z-Adda-D-Glu-Mdha], where the type of amino acid at each position in the cyclic heptapeptide varies (Abdallah et al., 2021; Baliu-Rodriguez et al., 2022). To date, more than 279 isomers have been found in water bodies, ranging in molecular weight from 881 to 1360 Da (Abdallah et al., 2021). These isomers have different degree of water contamination and toxicity among which, microcystin-LR (MC-LR), microcystin-RR (MC-RR), microcystin-YR (MC-YR) are the most common and toxic (Baliu-Rodriguez et al., 2022; Bouaicha et al., 2019). In addition, Mdha moiety is another key toxicity group, in which the unsaturated carbonyl group could be conjugated with glutathione to increase its toxicity to animals (Buratti and Testai 2015; Guo et al., 2015). Considering the exposure risk of MCs to humans, the WHO set a regulatory limit of 1.0 μg/L for MC-LR in drinking water (WHO 2003; WHO 2008). Therefore, in order to protect human health and monitor the pollution of MCs in fresh water, it is necessary to establish sensitive and accurate quantitative analytical methods for routine analysis (Preece et al., 2017; Xu et al., 2020; Yao et al., 2021).

In recent years, LC-MS/MS has become the first choice in routine analysis for quantitative determination of MCs because of its high sensitivity, high selectivity, and high throughput (Di Pofi et

al., 2020; Jimenez et al., 2020; Tran et al., 2020; Zhang et al., 2020b). The preparation of calibration curves is a key step for accurate quantification during the development of any LC-MS/MS method (Gu et al., 2014). In the past decades, the traditional multi-samples external calibration curves (MSCC) is a well-established approach, which has been widely adopted for algae toxins analysis (Di Pofi et al., 2020; Haddad et al., 2019; Tran et al., 2020; Turner et al., 2018; Zhang et al., 2020a). However, MSCC has some drawbacks. For example, each batch of samples needs to prepare at least six blank matrix samples spiked with different concentrations, and samples of different matrixes need to prepare corresponding MSCCs respectively (Kruve et al., 2015; Trufelli et al., 2011). At the same time, the preparation of multiple calibration curve points requires high proficiency of test personnel, which severely limits the speed and throughput of quantitative analysis methods (Chiva et al., 2019; Gu et al., 2019a). In order to eliminate the matrix effect between different samples and improve the accuracy of the quantitative results in the quantitative analysis of MCs by LC-MS/MS, it is usually necessary to adopt complex sample pre-processing steps, such as solid-phase extraction purification and other purification methods (Haddad et al., 2019; Jimenez et al., 2020; Massey et al., 2020; Turner et al., 2018). The use of internal standards (IS) in both external calibration curves and study samples can significantly improve the operational errors during sample preparation and instrument testing, thereby improving the accuracy of LC-MS/MS quantitative results (Kruve et al., 2015; Tran et al., 2020). Previously, the IS has been widely used in the quantitative analysis of small molecule compounds and peptides, but until recent, the use of ^{15}N-labeled isotope internal standards for the quantification of MCs in freshwater is reported (Tran et al., 2020). However, in the summer and autumn of cyanobacteria blooms, daily monitoring of freshwater samples by analytical laboratories is required, and this necessities higher requirements on the throughput of analytical

methods. Although MSCC has the advantages of accurate quantification, the configuration is more cumbersome, in contrast, single-point calibration (SPC) strategy only needs to configure one concentration, the configuration is simple and convenient, but the quantitative accuracy of SPC is poor which can only provide relative quantitation (Fornal and Stachniuk 2012). To improve the throughput of the analytical method, analysts do not do any pre-processing on some relatively clean fresh water samples, and direct injection technique (DI) was used for analysis (Zhang et al., 2020a). In view of the advantages and disadvantages of MPC and SPC, it is needed to develop a new calibration curve configuration strategy for the high-throughput and high-accuracy quantitative analysis of MCs in freshwater.

Recently, a new approach using the natural isotopic distribution of compounds or IS to generate multipoint calibration curves in only one sample is proposed by several studies, which eliminated the preparation of MSCC curve, improved throughput and is suitable for quantitative analysis of compounds and peptides (Chiva et al., 2019; Gu et al., 2019a; Gu et al., 2019b; Maus et al., 2021). In the development of traditional LC-MS/MS analytical methods, isotope peaks are usually regarded as useless information (Gu et al., 2019a). In fact, the isotope peak distribution of each compound is relatively fixed and is only related to the elemental composition of the compound. In general, the number of C atoms in a compound has the greatest influence on the number and abundance of isotope peaks, followed by N and O atoms, because the ratios of $^{13}C/^{12}C$, $^{15}N/^{14}N$, $^{18}O/^{16}O$, $^{17}O/^{16}O$, and $^{2}H/^{1}H$ are 1.1%, 0.36%, 0.2%, 0.04%, and 0.015%, respectively. Therefore, a compound with a larger molecular weight has a better number and intensity of isotope peaks, which is more conducive to using isotope peaks to construct a multi-point calibration curve in one sample (Gu et al., 2019a; Sun et al., 2022). Up to now, limited research documented that the application of isotopologue

multipoint calibration (IMC) for samples analyses, which mainly focus on the quantitative bioanalysis of peptide drugs in serum or tissues (Gu et al., 2019a) (Chiva et al., 2019; Gu et al., 2019b; Ibrahim et al., 2020; Zheng et al., 2020). Recently, it was reported that the multipoint calibration curve could be generated using multiple isotopologue reaction monitoring (MIRM) of analytes or IS by LC-MS/MS (Gu et al., 2019a; Gu et al., 2019b). Additionally, according to the isotopic abundances of fragment ions and neutral loss, the theoretical isotopic abundances of analytes for each MIRM channels could be accurately calculated (Gu et al., 2019a). When MIRM is applied to compound or stable isotope IS, one sample multipoint external calibration curve (OSCC) and in sample calibration curve (ISCC) can be generated, respectively (Gu et al., 2019a; Gu et al., 2019b). However, the development and application of the IMC strategy is in the initial stage, and in-depth research is still needed (Visconti et al., 2022; Yuan et al., 2020). In this study, eight MCs variants were chosen to discuss the feasibility, advantages and disadvantages of different IMC strategies in the quantitative analysis, and to present an in-depth comparison with traditional calibration curve strategies. The research results provide a new strategy for the high-throughput quantitative analysis of MCs in freshwater, and at the same time provide a reference for expanding the application of the IMC strategies in water and food analysis as well as other fields.

2. Materials and methods

2.1. Chemicals, reagents and stock solutions

A total of eight MCs variants are investigated in this study, including MC-LR, MC-RR, MC-YR, MC-WR, MC-LA, MC-LY, MC-LW, and MC-LF. The standards for these eight MCs were purchased from Enzo Life Sciences (Farmingdale, USA) with the purity>98%. In addition, high purity (>98%)

^{15}N-labeled isotope IS solutions for the same targeted MCs, including $^{15}N_{10}$-MC-LR, $^{15}N_{13}$-MC-RR, $^{15}N_{10}$-MC-YR, $^{15}N_{11}$-MC-WR, $^{15}N_{7}$-MC-LA, $^{15}N_{7}$-MC-LY, $^{15}N_{8}$-MC-LW, and $^{15}N_{7}$-MC-LF, were purchased from Cambridge Isotope Laboratories, Inc. (Tewksbury, USA). Individual stock solutions of 1,000 µg/L of the targeted toxins were prepared in pure methanol and stored in the dark at -20 ^{o}C for a maximum of one year. For working solutions (10 µg/L), they were prepared from the stock solutions in pure methanol and stored at 4 ^{o}C, which were renewed monthly. For the internal standards solutions, they were diluted with pure methanol before they were spiked in samples. Other chemical reagents and solvents were all MS grade, such as acetonitrile, methanol, and formic acid, and they were obtained from Thermo Fisher (Harnover Park, USA). Finally, ultra-pure water was obtained from a Milli-Q water system (18.2 mΩ, Bedford, USA).

2.2. Freshwater lake samples collection and preparation

Ten blank freshwater lake samples were collected from Chaohu Lake (Hefei, China; n=5) and Lake Tai (Suzhou, China; n=5) during the spring season (March, 2021), which were used for the method optimization and validation. The collected blank samples were free of MCs, in which no peaks of the targeted analytes were observed. Surface lake water samples were collected during the autumn season (October, 2021) which consist of twenty lake water samples from Chaohu Lake (n=10) and Lake Tai (n=10). All samples were collected in one liter amber glass bottles, transported to the lab within 24 h at room temperature and stored at 4 ^{o}C under dark condition once delivered to the lab. Extraction of MCs from water was done using simple and straightforward method. From each sample, 1.2 mL were transferred into 1.5 mL microcentrifuge tubes and were frozen at -20 ^{o}C for 20 min and then thawed at the room temperature. This step was repeated three times and then sonicated for 10 min, centrifuged at 12,000 *g* for 10 min and filtered with 0.22 µm membrane filters. Finally,

980 µL of water samples with 20 µL isotopically labelled internal standards were transferred into 2 mL glass vials for further LC-MS/MS analysis.

2.3. Liquid chromatography tandem mass spectrometry (LC-MS/MS) conditions

UHPLC (Agilent 1290 Infinity II system, USA) coupled to a triple quadrupole mass spectrometer (MS/MS, Agilent 6495, USA) equipped with a Dual Agilent Jet Stream ESI (Agilent, USA). Selective reaction monitoring (SRM) under positive ionization mode was adopted for MS data acquisition, and the MassHunter software (Agilent, USA) was used for data process. The ESI parameters are set as follow: electrospray capillary, 4.0 kV; the sheath gas temperature and flow were 400 ^{o}C and 12 L/min, respectively; the gas temperature and flow were 290 ^{o}C and 5 L/min, respectively. The precursor and product ions were selected for monitoring all analytes. And the MRM and MIRM parameters for each MCs are available in **Table S1**, **S2** and **Table 1**, respectively. Chromatographic separation of microcystins was carried out on Poroshell 120 EC-C18 column (2.1 × 100 mm, 2.7 µm; Agilent, USA) using a gradient elution of solvent A (ultra-pure water contains 0.1% formic acid) and solvent B (acetonitrile contains 0.1% formic acid) as follows: 0.0-0.50min, 30% B; 0.5-3.5 min, 30% B to 40% B; 3.5-5.5 min, 40% B to 85% B; 5.5-6.0 min, 85% B to 100% B and maintained for 0.40 min; 6.4-7.5 min, 30% B. The column temperature was keep at 40 ^{o}C during the analysis, and the injection volume was set at 20 µL.

2.4. Preparation of calibration curves for MSCC, OSCC and ISCC.

Three different types of calibration curves were prepared in this study, namely: (A) traditional MSCC; (B) OSCC; and (C) ISCC. For the preparation of MSCC, the standard working solution was diluted at six different concentration levels using the blank lake water, in which the concentration levels were set as 0.05, 0.1, 0.25, 1.0, 5.0, and 10.0 µg/L for MC-LR, MC-RR, MC-YR, and

MC-WR, while 0.5, 1, 2.5, 10, 50, and 100 µg/L for MC-LA, MC-LY, MC-LW, and MC-LF. And 1 or 10 µg/L SIL-IS was spiked in each calibration samples. Two MRM transitions for each MC were selected for quantification and confirmation, and one transition for SIL-IS, which was available for MRM parameters in **Table S1**. For OSCC, only one concentration level of 10 or 100 µg/L was prepared in blank freshwater lake with 1 or 10 µg/L SIL-IS for each microcystin. Six different MIRM transitions were selected to build the OSCCs with six levels from 0.064 to 10 µg/L for MC-LR, MC-RR, MC-YR, and MC-WR; and 0.64 to 100 µg/L for MC-LA, MC-LY, MC-LW, and MC-LF, and the detail MIRM transitions is provided in **Table 1**. While for ISCC, we only prepared 10 or 100 µg/L SIL-IS in the study samples by appropriate dilution. Similarly, the calibration curve was built by monitoring six MIRM channels of SIL-IS (**Table S2**) in each study sample. Origin software was used to compute the obtained data. The line regression was established by plotting the ratio of peaks area between MCs and their SIL-ISs over the analyte concentration range for MSCC and OSCC, while for ISCC, the peaks areas of six MIRM channels of SILs versus the concentration was plotted. The concentration level of MCs in samples could be back to calculate it using the established calibration curve.

2.5. Method validation

A mixture of the ten blank lake water samples (MCs free) was used for the validation study following the recommendation of European Commission Regulation No. 401/2006/EC criteria (Commission 2002; Commission 2006). The following parameters: matrix effect, selectivity, sensitivity, accuracy, and precision were carefully evaluated in this study. One concentration level of standards was spiked to blank lake water sample and pure solvent (Milli-Q ultra-water) to assess the matrix induced signal suppression and enhancement. In addition, the limits of detection (LODs) and

limits of quantification (LOQs) were determined from spiked blank samples with a signal to noise (S/N) ratio being more than 3 and 10, respectively. Furthermore, accuracy and precision were calculated by spiking standards to blank samples at three different concentration levels of 0.1, 0.3 and 1.0 μg/L for MC-LR, MC-RR, MC-YR, and MC-WR; and 1, 3 and 10 μg/L for MC-LA, MC-LY, MC-LW, and MC-LF. Six replicates at three spiked levels were carried out to obtain the accuracy values. For the precision, the intra-day precision and inter-day precision were evaluated calculating the relative standard deviation (RSD) of eighteen replications from three bathes, which were analyzed by LC-MS/MS on the same day and three different days.

3. Results and discussion

3.1. Optimization of MIRM channels for OSCC and ISCC for the quantitative analysis of eight MCs by LC-MS/MS.

The preparation of calibration curves is a critical step in developing a quantitative LC-MS/MS method, which significantly affects the accuracy and precision of the analysis (Gu et al., 2014; Gu et al., 2019b; Maus et al., 2021). However, the traditional MSCC strategy (**Fig. 1A**) requires the configuration of six different concentrations, which is time-consuming and labor intensive (Gu et al., 2019b). Currently, more than hundred variants of MCs have been reported, and even the frequently tested types of MCs are more than a dozen (Baliu-Rodriguez et al., 2022; Massey et al., 2020). For a high throughput analysis, configuration of calibration curve would be cumbersome. The IMC strategy is a good alternative to tackle the above-mentioned issue, since OSCC (**Fig. 1B**) could fulfill the plot of the calibration curve using a single sample, while ISCC (**Fig. 1C**) incorporates the calibration curve into each study sample (Gu et al., 2019a; Gu et al., 2019b; Sun et al., 2022). The

matrix effects of different freshwater lakes are quite different, which will significantly affect the accuracy of the analytical method used for analysis. However, the introduction of SIL-IS can effectively eliminate the errors during sample pretreatment and analysis (Stokvis et al., 2005; Tran et al., 2020). Deuterium, ^{13}C and ^{15}N labelling are the commonly used methods for isotopic internal standards, where the Deuterium-labelled IS has the potential for H/D exchange, thus affecting the accuracy of the analytical results (Stokvis et al., 2005). Therefore, ^{13}C and ^{15}N-labelled IS are preferred for MCs (Stokvis et al., 2005). The natural isotopic peaks of MCs are mainly derived from elemental C (1.1% for $^{12}C/^{13}C$), while other elements contribute less to the isotope. As for the ^{13}C-labelled IS, normally all the C elements in the MCs molecule are replaced by ^{13}C, resulting in significant changes in the isotopic peak profiles of precursor compared to unlabeled form, especially the number and abundance of the isotopic peaks are significantly lower, thus making it difficult to achieve IMC (Sun et al., 2022). In contrast, the ^{15}N labelled IS of MCs have a minor effect on the profile of its isotopic peaks. As the ISCC strategy mainly uses IS and its isotopic peaks to plot calibration curves, ^{15}N-labelled IS was selected for the quantitative analysis of MCs in this study. The *m/z* value of ^{15}N-labelled IS has a slight shift compared to the prototype, but no change in its physical or chemical properties. In theory, the ^{15}N-labelled IS and the prototype are supposed to have exactly the same chromatographic behavior and mass spectral signal intensity (Jimenez et al., 2020; Visconti et al., 2022). However, slight difference in the chromatographic and spectrometric behavior was observed between the eight MCs and their SIL-ISs in the current study. In addition, given the quality of the IS product and the error in solution preparation, the ratio of MCs to the IS is preferable for the quantitative analysis. **Fig. 3B** shows the ratios and errors of eight different MCs and their SIL-IS (1 μg/L) in neat solution and matrix, and the difference in signal response on the mass spectra

and the matrix effect could be eliminated using the ratio method.

Generally, two SRM channels are selected for each compound in traditional MSCC strategy, where one for quantitative analysis and another for qualitative analysis (Tran et al., 2020; Zhang et al., 2020a). For SIL-IS, the quantitative fragment ion would be selected corresponding to its prototype, and the detailed MRM channels for the eight MCs and their ^{15}N-labled IS are available in **Table S1**. The precursors of MC-LR, MC-RR, MC-YR and MC-WR tending to form $[M+2H]^{2+}$ and $[M+3H]^{3+}$ during ESI^{+}, since arginine (R) are present in their chemical structure (**Fig. 2A**), and the high abundances of $[M+2H]^{2+}$ was used as the precursor ion for these four MCs in this study (Baliu-Rodriguez et al., 2022). Although numerous fragment ions were obtained for MCs under collision-induced dissociation (CID) of tandem MS, the fragment ion *m/z* 135.1 ($C_9H_{11}O^{+}$) from the Adda acid normally has the strongest ion intensity in most MCs, which is used as a quantitative ion in this study (Massey et al., 2020; Tran et al., 2020; Turner et al., 2018; Zhang et al., 2020b). In the IMC strategy, the mass spectra of MCs and their ^{15}N-labelled IS are used for calibration curves of OSCC and ISCC, respectively. During the selection and optimization of the MIRM channels, the mutual interference between the base peak and the isotope peak should be minimized; otherwise the signal ratio between the different MIRM channels will deviate from the theoretical value, leading to the inaccurate quantification of the IMC (Gu et al., 2019a; Gu et al., 2019b). In the QqQ, Q1 and Q3 belong to the unit resolution mass analyser and the optimum half-peak width obtained is 0.7 Da. With an isolation window of 0.7 Da, there is essentially no interference between the MIRM channels between the base peaks of $[M+H]^{+}$ and $[M+2H]^{2+}$ precursor ions and the isotope peaks. However, the signal ratio between the various MIRM channels can deviate significantly from the theoretical value for $[M+3H]^{3+}$. Therefore, in this study, only their single- and double-charged precursor ions were

selected as the MIRM channels of MCs. **Fig. 3A** described in detail the precursor ions of different charges in unit isolation window, quantitative ion *m/z* 135.1 and its isotopic peak ion intensity.

The selection of MIRM channels is a critical step for OSCC and ISCC strategies, which significantly affect the linear range, accuracy and precision of the developed method (Gu et al., 2019a; Gu et al., 2019b). To ensure the linear relationship of the calibration curve, the settings of mass spectrometry data acquisition parameters including collision energy and dwell time in all MIRM channels should be keep in consistent (Gu et al., 2019a). The isotopic abundances in each MIRM channel could be calculated based on the elemental composition of quantitative ions and the neutral loss groups, which have been reported by Gu et al., (Gu et al., 2019a). The isotopic distribution and elemental composition of the neutral loss groups and quantitative ions of the eight MCs and their ^{15}N-labled IS were in detail shown in **Table 2**. Taking the MC-LR as an example, about ten MIRM channels of MC-LR were assessed including 498.3→135.1 (100%); 498.8→136.1 (9.9%); 498.8→135.1 (48.11%); 499.3→137.1 (0.64%); 499.3→136.1 (4.76%); 499.3→135.1 (13.54%); 499.8→138.1 (0.03%); 499.8→137.1 (0.31%); 499.8→136.1 (1.34%); and 499.8→135.1 (2.76%), which is indicated in **Table S3** in detail. In fact, it is not necessary to adopted all the potential MIRM channels in the final assay, in which six data points meet the requirements of calibration curve. However, several considerations should be noted in the screening of MIRM channels: the isotopic abundance of each MIRM channels are fixed, and when there are MIRM channels with similar abundance ratios, only one of them needs to be retained. Additionally, the selected MIRM channels should be covered the expected concentration range. Furthermore, some MIRM channels have large variances between measured and theoretical values, which should be not considered. The calculated and measured relative isotopic abundance of the ten MIRM channels for

eight MCs and their ^{15}N-labled ISs at 10.0 μg/L were shown in **Table S3** and **Tables S4**, respectively. The observed error in some MIRM channels being greater than 20% should be removed in final assay, since there may be interference from endogenous substances in this MIRM channel. Finally, *m/z* 498.3→135.1 (100%); 498.8→135.1 (48.11%); 499.3→135.1 (13.54%); 499.3→136.1 (4.76%); 499.8→136.1 (1.34%); and 499.3→137.1 (0.64%), were used for constructing OSCC of MC-LR, which have 156.25-fold curve range for MC-LR. Since the quantitative ions (*m/z* 135.1) of the eight MCs are all from fragment ions of Adda acid, and thus the setting of MIRM channels for the other seven MCs were approximately the same as MC-LR. The detailed MIRM channels and typical MIRM chromatograms for eight MCs are available in **Table 1** and **Fig. 2B**, respectively. In the development of the ISCC method, the calibration curve was built based on the MIRM channels of ^{15}N-labled IS. The MIRM channels were selected and optimized in the same manner as for the OSCC configuration, also using *m/z* 135.1 as the quantitative ion. Taking ^{15}N-labled MC-LR as an example, *m/z* 503.3→135.1 (100%); 503.8→135.1 (44.42%); 504.3→135.1 (13.54%); 504.3→136.1 (4.4%); 504.8→136.1 (1.34%); and 504.3→137.1 (0.64%) were used for the ISCC configuration. Details of eight ^{15}N-labled MCs MIRM channels settings were shown in **Table S2**. To ensure that the ISCC of configuration has suitable quantitative range, the ^{15}N-labled MCs concentration used should be significantly higher than its concentration when used as an internal standard at OSCC and MSCC. In addition, compared to MRM, the number of MIRM channels has increased more than three-fold, and in order to have enough data point for each peak, dynamic MS data acquisition was adopted and the detection time window was set at 1 min. Furthermore, the appropriate gradient elution procedure should be chosen when developing the chromatographic method to separate the peak retention times of each MCs.

3.2. Comparing the method validation and performance of the three strategies (MSCC, OSCC and ISCC) in quantitation the eight MCs.

To evaluate the quantitative performance of the proposed OSCC and ISCC approaches for the MCs analysis, a validation was performed by spiking three different levels of MCs in blank freshwater lakes in terms of sensitivity, accuracy and precision. In the traditional MSCC, the concentration of each point in the calibration curve could be adjusted according to the operator's needs. However, the curve points and range of OSCC and ISCC are defined by the isotopic abundance of the selected MIRM channels, where the most and less abundant MIRM channels were served as the assay upper and lower limit of quantitation (Gu et al., 2019a; Gu et al., 2019b). In the current study, the selected MIRM channels have about 160-fold curve range for eight MCs in both novel approaches. Additionally, a least-squares linear regression without weight was adopted for both OSCC and ISCC. **Fig. 3C** showed the errors between the theoretical and measured values at each point for the eight MCs for the three different calibration curve strategies. The error values for each data point on the OSCC and ISCC calibration curves constructed on the basis of MIRM are significantly less than those for MSCC, especially at low concentration, where MSCC presents larger error values, with some data values higher than 20%. This is mainly due to the fact that the isotopic abundances in each MIRM channel are established based on the natural isotopes of the compounds and do not involve variation in MSCC solution preparation and instrumental detection (Gu et al., 2019a; Gu et al., 2019b). The sensitivity of MCs is mainly related to the settings of the mass spectrometry data acquisition parameters, but correlated to the calibration curve. The three calibration curves used in this study are basically identical in the settings of the parameters of precursor ions, daughter ions and collision energies in MRM channels. Therefore, the three methods

have exactly the same sensitivity for MCs. However, the LOQ for the three strategies were slightly different, and the LOQ for MSCC, OSCC and ISCC were 0.05, 0.064 and 0.064 ng/mL for eight MCs, respectively. In comparison with the recent reported methods, the sensitive of the proposed method was quite excellent, which could well meet the requirement for investigating the containment of MCs in freshwater (Liu et al., 2022; Liu et al., 2021). Furthermore, the linearity range, correlation coefficient (r^2) of calibration curve, LODs and LOQs for eight MCs under three different approaches are provided in **Table 3**. Additionally, the recovery and precision of three different calibration curve methodology were evaluated by spiking targeted MCs to blank freshwater lakes at three different concentration levels of 0.1, 0.3, and 1.0 μg/L, and the obtained results was indicated in **Fig. 4** in detail. Overall, the OSCC and ISCC based on the MIRM strategy showed outperformed as the traditional MSCC in terms of accuracy and precision, especially at low concentration levels (0.1 μg/L), where the coefficient of variation was more than 15% for some MCs. It should be pointed out that the error-prone steps of preparation of multi-sample external calibration curves, and sample analysis from individual samples have been eliminated in OSCC and ISCC approaches. The obtained results demonstrate that the OSCC and ISCC approaches exhibited excellent performances in linearity, sensitivity, accuracy, precision and stability for the quantitation of MCs in freshwater. Additionally, the preparation of calibration curve is substantially time-saving in comparison to conventional MSCC, which in turn improves the throughput and efficiency of the analytical method.

3.3. Application to the freshwater lake samples collected from Lake Tai and Chaohu Lake.

A total number of twenty freshwater lake samples were collected from Lake Tai and Chaohu Lake in autumn, when MCs are mostly present in water (Li et al., 2022). To assess the MCs contamination, three different calibration curve methods were used to detect and quantify MCs in the

collected freshwater samples, and the measured values is almost the same, in which the errors is less than 8.7% among three different calibration curves. **Table 4** described the contamination of the eight MCs in the 20 samples using OSCC approach, showing that MC-LR, MC-RR and MC-YR were the three most contaminating toxins in the lake water, while other toxins were also detected with significantly lower concentrations. In addition, due to the large area of Lake Tai and Chaohu Lake, the concentrations of MCs in freshwater samples collected from different locations were also significantly different. There were two samples collected from Chaohu Lake were greater than 1.0 μg/L for MC-LR, implying that the problem of MCs contamination in lake water should arise more attention. Moreover, the concentration of contaminated MCs in the lake water is highly variable, even up to 12.4 μg/L of RR in one sample collected in the present study, which is beyond the upper limit of quantification (ULOQ). In order to obtain accurate quantitative analysis results, the dilution of high concentration samples is inevitable, and the dilution and reanalysis steps for highly concentrated samples are cumbersome, time-consuming and error-prone, thus affecting the throughput and accuracy of the analytical method (Gu et al., 2019a; Maus et al., 2021). Like the conventional MSCC, OSCC needs to use the blank matrix-matched external calibration curve, whereas the difference is that the OSCC strategy requires the simultaneous determination of multiple MIRM channels, where only the channel with the highest intensity of MIRM channels is used for quantitative analysis while the other collected MIRM channels are usually discarded as invalid information. In fact, the isotopic abundance of each MIRM channel can be precisely calculated and measured, and these less abundant MIRM channels could be served as the quantitation channels, especially for the samples having high concentration beyond the ULOQ. In this case, the signal intensity information of less abundant MIRM channels can be multiplied by the isotope peak dilution

366 factor to accurately quantify the MCs in highly concentrated samples beyond ULOQ without the
367 need for sample dilution and re-analysis(Gu et al., 2019a; Maus et al., 2021). However, there is a
368 strict range of dilution factors based on isotope peaks to achieve dilution-free quantitative analysis of
369 highly concentrated samples. Our results indicated that the accuracy and precision fully meet the
370 needs of quantitative analysis when the dilution factor is within ten-fold. When the dilution factor is
371 higher than ten, the accuracy of the quantification results is significantly decreased. This is mainly
372 due to the fact that the ionization of MCs at different concentrations is not completely linear at ESI,
373 especially at higher concentrations where the ionization efficiency of the compounds is significantly
374 reduced (Gu et al., 2014). Therefore, the range of dilution factors should be systematically assessed
375 when using OSCC to accurately quantify highly concentrated samples.

376 *3.4. The potential applications and improvements of OSCC and ISCC strategies.*

377 The current work demonstrated an excellent performance of OSCC and ISCC in MCs
378 quantitation in freshwater with good accuracy and stability, and reducing the need to prepare
379 multiple samples in the traditional MSCC. The addition of SIL-IS to the calibration curve and study
380 samples effectively eliminated the variation between samples during sample pretreatment and
381 LC-MS/MS analysis, which further improved the accuracy and stability of the analytical method.
382 During the preparation of ISCC, a high concentration of SIL-ISs is needed to obtain a suitable
383 ULOQ (Gu et al., 2019b; Yuan et al., 2020; Zheng et al., 2020). However, SIL-ISs is normally very
384 expensive, which raises the cost of analytical method for ISCC. By comparison, only trace levels of
385 SIL-ISs are used in OSCC approach, which therefore offers a greater economic advantage over ISCC
386 in terms of analytical costs (Gu et al., 2019a; Maus et al., 2021). Furthermore, the OSCC essentially
387 retains various advantages of the ISCC analysis, which eliminates the need to prepare multiple

external samples for the traditional MSCC and allows the calibration curve to be configured with a single sample. In addition, OSCC eliminates the need to dilute and re-analyze samples at high concentrations and enables accurate quantification of target compounds by monitoring the less abundance MIRM channel. Nevertheless, the ISCC strategy avoids the need for external calibration curves and blank samples, especially when the blank matrix is not available, making the ISCC strategy as the only selection (Gu et al., 2019b; Visconti et al., 2022). In both OSCC and ISCC, six MIRM channels are required for each compound, while the less abundant MIRM channels are susceptible to interference from endogenous material in the matrix. It is of great importance to optimize the chromatographic elution procedures and enhance the sample pre-treatment methods to minimize the interference. However, the strict requirement would increase the difficulty of developing analytical methods and reduce their usefulness. A hyperbolic quadrupole mass spectrometry or ion trap with higher quality separation performance could reduce the interference of endogenous substances in the matrix to the low abundance MIRM channels by defining a relatively narrow isolation window, thereby enhancing the sensitivity. The ratios between MIRM channels can be accurately calculated based on the elemental composition of the neutral loss groups and quantitative ions, and further to plot the OSCC and ISCC. However, the data analysis relies on analysts using offline software, which severely hinders the application of the strategy in various fields. Currently, OSCC and ISCC have been successfully applied in drug development and clinical diagnosis (Gu et al., 2019b; Visconti et al., 2022; Yuan et al., 2020; Zheng et al., 2020), making them promising strategies to be applied in many other fields such as food analysis, environmental analysis and medicinal analysis, when the corresponding MIRM data-mining techniques integrated into the analytical software.

4. Conclusions

In summary, a novel one-point calibration approach including OSCC and ISCC based on MIRM technology is proposed for the quantitation of eight MCs in freshwater using LC-MS/MS. In comparison with the traditional MSCC, this strategy exhibited good performance in selectivity, sensitivity, accuracy and precision. Furthermore, the proposed one-point calibration approach was successfully investigated the contamination of MCs in freshwater lake samples collected in two major lakes in China. Considering the advantages of excluding the MSCC preparation, simplified workflows and improved throughput, OSCC and ISCC will be favored for MCs monitoring and as an emerging approach in environmental pollutant control analysis and prevention.

CRediT authorship contribution statement

Huiyan Zhang: Conceptualization, data curation, methodology and writing the original draft. **Yanshen Li**: data curation, and methodology. **Mohamed F. Abdallah**: writing and revising the draft. **Jianxun Li, Shuyan Liu, and Rong Zhang**: methodology and revising the draft. **Feifei Sun**: writing and revising the draft. **Yi, Li:** Supervision. **Shupeng Yang**: Supervision, conceptualization and funding acquisition.

Declaration of Competing Interest

The authors declare that there is no conflict of interest.

Acknowledgments

We thank the financial support from the National Science Foundation of China (No.31702296).

Appendix A. Supplementary data

The MRM and MIRM parameters for eight MCs and SIL-ISs used for the constructing MSCC and ISCC are available in **Table S1** and **Table S2**, respectively. And the theoretical and measured relative isotopic abundances in MIRM channels for eight MCs and SIL-ISs for OSCC and ISCC are indicated in **Table S3** and **Table S4**, respectively.

References

Abdallah, M. F., Van Hassel, W. H. R., Andjelkovic, M., Wilmotte, A., Rajkovic, A., 2021. Cyanotoxins and food contamination in developing countries: review of their types, toxicity, analysis, occurrence and mitigation strategies. Toxins, 13. https://doi:10.3390/toxins13110786

Baliu-Rodriguez, D., Peraino, N. J., Premathilaka, S. H., Birbeck, J. A., Baliu-Rodriguez, T., Westrick, J. A., Isailovic, D. (2022). Identification of novel microcystins using high-resolution MS and MSn with Python code. Environ. Sci. Technol. 56, 1652-1663. https://doi:10.1021/acs.est.1c04296

Bouaicha, N., Miles, C. O., Beach, D. G., Labidi, Z., Djabri, A., Benayache, N. Y., Nguyen-Quang, T., 2019. Structural diversity, characterization and toxicology of microcystins. Toxins. 11. https://doi:10.3390/toxins11120714

Buratti, F. M., Testai, E., 2015. Species- and congener-differences in microcystin-LR and -RR GSH conjugation in human, rat, and mouse hepatic cytosol. Toxicol. Lett. 232, 133-140. https://doi:10.1016/j.toxlet.2014.10.020

Chiva, C., Pastor, O., Trilla-Fuertes, L., Gamez-Pozo, A., Vara, J. A. F., Sabido, E., 2019. Isotopologue multipoint calibration for proteomics biomarker quantification in clinical practice. Anal. Chem. 91, 4934-4938. https://doi:10.1021/acs.analchem.8b05802

Commission E., 2002. Commission decision 2002/657/EC implementing council directive 96/23/EC concerning the performance of analytical methods and the interpretation of results, OJ L221/8-36.

Commission E., 2006. Commission regulation 401/2006/EC of 23 february 2006 laying down the methods of sampling and analysis for the official control of the levels of mycotoxins in foodstuffs, OJ L 70/12-34.

Di Pofi, G., Favero, G., Di Gregorio, F. N., Ferretti, E., Viaggiu, E., Lucentini, L., 2020. Multi-residue ultra performance liquid chromatography-high resolution mass spectrometric method for the analysis of 21 cyanotoxins in surface water for human consumption. Talanta 211. https://doi:ARTN 12073810.1016/j.talanta.2020.120738

Fornal, E., Stachniuk, A., 2012. Application of a truly one-point calibration for pesticide residue control by liquid chromatography-mass spectrometry. J. Chromatogr. B 901, 107-114. https://doi:10.1016/j.jchromb.2012.06.014

Gu, H. D., Liu, G. W., Wang, J., Aubry, A. F., Arnold, M. E., 2014. Selecting the correct weighting factors for linear and quadratic calibration curves with least-squares regression algorithm in bioanalytical LC-MS/MS assays and impacts of using incorrect weighting factors on curve stability, data quality, and assay performance. Anal.

Chem. 86, 8959-8966. https://doi:10.1021/ac5018265

Gu, H. D., Zhao, Y., DeMichele, M., Zheng, N. Y., Zhang, Y. J., Pillutla, R., Zeng, J. N., 2019a. Eliminating preparation of multisample external calibration curves and dilution of study samples using the multiple isotopologue reaction monitoring (MIRM) technique in quantitative LC-MS/MS bioanalysis. Anal. Chem. 91, 8652-8659. https://doi:10.1021/acs.analchem.9b02136

Gu, H. D., Zhao, Y., DeMichele, M., Zheng, N. Y., Zhang, Y. J., Pillutla, R., Zeng, J. N., 2019b. In-sample calibration curve using multiple isotopologue reaction monitoring of a stable isotopically labeled analyte for instant LC-MS/MS bioanalysis and quantitative proteomics. Anal. Chem. 91, 2536-2543. https://doi:10.1021/acs.analchem.8b05656

Guo, X. C., Chen, L., Chen, J., Xie, P., Li, S. C., He, J., Li, W., Fan, H. H., Yu, D. Z., Zeng, C., 2015. Quantitatively evaluating detoxification of the hepatotoxic microcystin-LR through the glutathione (GSH) pathway in SD rats. Environ. Sci. Pollut. R. 22, 19273-19284. https://doi:10.1007/s11356-016-6081-y

Haddad, S. P., Bobbitt, J. M., Taylor, R. B., Lovin, L. M., Conkle, J. L., Chambliss, C. K., Brooks, B. W., 2019. Determination of microcystins, nodularin, anatoxin-a, cylindrospermopsin, and saxitoxin in water and fish tissue using isotope dilution liquid chromatography tandem mass spectrometry. J. Chromatogr. A 1609. https://doi:10.1016/j.chroma.2019.03.066

Harke, M. J., Steffen, M. M., Gobler, C. J., Otten, T. G., Wilhelm, S. W., Wood, S. A., Paerl, H. W., 2016. A review of the global ecology, genomics, and biogeography of the toxic cyanobacterium, Microcystis spp. Harmful Algae 54,4-20 https://doi:10.1016/j.hal.2015.12.007

Ibrahim, S., Froehlich, B. C., Aguilar-Mahecha, A., Aloyz, R., Poetz, O., Basik, M., Batist, G., Zahedi, R. P., & Borchers, C. H., 2020. Using two peptide isotopologues as internal standards for the streamlined quantification of low-abundance proteins by immuno-MRM and immuno-MALDI. Anal. Chem. 92, 12407-12414. https://doi:10.1021/acs.analchem.0c02157

Janssen, E. M. L., 2019. Cyanobacterial peptides beyond microcystins - A review on co-occurrence, toxicity, and challenges for risk assessment. Water Res. 151,488-499. https://doi:10.1016/j.watres.2018.12.048

Jimenez, L. D. Q., Guzman-Guillen, R., Catunescu, G. M., Campos, A., Vasconcelos, V., Jos, A., Camean, A. M., 2020. A new method for the simultaneous determination of cyanotoxins (Microcystins and Cylindrospermopsin) in mussels using SPE-UPLC-MS/MS. Environ. Res. 185. https://doi:ARTN 10928410.1016/j.envres.2020.109284

Kim, M., Kim, D., Kim, J., Hong, S., Shin, K. H., 2021. Distribution of microcystins in environmental multimedia

and their bioaccumulation characteristics in marine benthic organisms in the Geum River Estuary, South Korea. Sci. Total Environ. 757. https://doi:ARTN14381510.1016/j.scitotenv.2020.143815

Kruve, A., Rebane, R., Kipper, K., Oldekop, M. L., Evard, H., Herodes, K., Ravio, P., Leito, I., 2015. Tutorial review on validation of liquid chromatography-mass spectrometry methods: Part I. Anal. Chim. Acta. 870, 29-44. https://doi:10.1016/j.aca.2015.02.017

Li, H. M., Gu, X. H., Chen, H. H., Mao, Z. G., Shen, R. J., Zeng, Q. F., Ge, Y. 2022. Co-occurrence of multiple cyanotoxins and taste-and-odor compounds in the large eutrophic Lake Taihu, China: Dynamics, driving factors, and challenges for risk assessment. Environ. Pollut. 294. https://doi.org/10.1016/j.envpol.2021.118594

Liu J., Xing Y., Xue B., Zhou X. 2022. Nanozyme enhanced paper-based biochip with a smartphone readout system for rapid detection of cyanotoxins in water. Biosens. Bioelectron. 205, 114099. https://doi.org/10.1016/j.bios.2022.114099

Liu J., Yang Y., Zhu Q., Wang, Z., Hu, G., Shi, H., Zhou, X. 2021. ELISA-Based Method for Variant-Independent Detection of Total Microcystins and Nodularins via a Multi-immunogen Approach. Environ. Sci. Technol. 55, 12984-12993. https://doi.org/10.1021/acs.est.1c03330

Massey, I. Y., Wu, P., Wei, J., Luo, J. Y., Ding, P., Wei, H. Y., Yang, F., 2020. A mini-review on detection methods of microcystins. Toxins 12. https://doi:ARTN 64110.3390/toxins12100641

Maus, A. D., Kemp, J. V., Hoffmann, T. J., Ramsay, S. L., Grebe, S. K. G., 2021. Isotopic distribution calibration for mass spectrometry. Anal. Chem. 93, 12532-12540. https://doi:10.1021/acs.analchem.1c01672

Preece, E. P., Hardy, F. J., Moore, B. C., Bryan, M., 2017. A review of microcystin detections in Estuarine and Marine waters: Environmental implications and human health risk. Harmful Algae 61, 31-45. https://doi:10.1016/j.hal.2016.11.006

Stokvis, E., Rosing, H., Beijnen, J. H., 2005. Stable isotopically labeled internal standards in quantitative bioanalysis using liquid chromatography/mass spectrometry: necessity or not? Rapid Commun. Mass Sp. 19, 401-407. https://doi:10.1002/rcm.1790

Sun, F. F., Tan, H. G., Abdallah, M. F., Li, Y. S., Zhou, J. H., Li, Y.,Yang, S. P., 2022. A novel calibration strategy based on isotopic distribution for high-throughput quantitative analysis of pesticides and veterinary drugs using LC-HRMS. J. Hazard. Mater. 430. https://doi:ARTN 12841310.1016/j.jhazmat.2022.128413

Tran, N. H., Li, Y. W., Reinhard, M., He, Y. L., Gin, K. Y. H., 2020. A sensitive and accurate method for simultaneous analysis of algal toxins in freshwater using UPLC-MS/MS and N-15-microcystins as isotopically labelled internal standards. Sci. Total Environ. 738. https://doi:ARTN 13972710.1016/j.scitotenv.2020.139727

Trufelli, H., Palma, P., Famiglini, G., Cappiello, A., 2011. An overview of matrix effects in liquid chromatography-mass spectrometry. Mass Spectrom. Rev. 30, 491-509. https://doi:10.1002/mas.20298

Turner, A. D., Waack, J., Lewis, A., Edwards, C., Lawton, L., 2018. Development and single-laboratory validation of a UHPLC-MS/MS method for quantitation of microcystins and nodularin in natural water, cyanobacteria, shellfish and algal supplement tablet powders. J. Chromatogr. B 1074-1075, 111-123. https://doi:10.1016/j.jchromb.2017.12.032

Visconti, G., Olesti, E., Gonzalez-Ruiz, V., Glauser, G., Tonoli, D., Lescuyer, P., Vuilleumier, N., Rudaz, S., 2022. Internal calibration as an emerging approach for endogenous analyte quantification: Application to steroids. Talanta 240. https://doi:ARTN 12314910.1016/j.talanta.2021.123149

World health organisation report, 2003. Guidelines for safe recreational water environments.

World health organisation report, 2008. The world health report-guideline for drinking water quality.

Xu, Z. L., Ye, S. L., Luo, L., Hua, X., Lai, J. X., Cai, X. P., Liang, Q. W., Lei, H. T., Sun, Y. M., Chen, Y. P., Shen, X., 2020. Fluorescent enzyme-linked immunoassay based on silane-doped carbon dots for sensitive detection of microcystin-LR in water and crucian samples. Sci. Total. Environ. 708. https://doi:10.1016/j.scitotenv.2019.134614

Yao, L., He, L., Yang, Y., Zhang, Y., Liu, Z., Liang, L., Piao, Y., 2021. Nanobiochar paper based electrochemical immunosensor for fast and ultrasensitive detection of microcystin-LR. Sci. Total. Environ., 750. https://doi:10.1016/j.scitotenv.2020.141692

Yuan, L., Gu, H. D., Zeng, J. N., Pillutla, R. C., Ji, Q. C., 2020. Application of in-sample calibration curve methodology for regulated bioanalysis: Critical considerations in method development, validation and sample analysis. J. Pharmaceut. Biomed. 177. https://doi:ARTN 11284410.1016/j.jpba.2019.112844

Zhang, H. Y., Gonzales, G. B., Beloglazova, N. V., De Saeger, S., Shen, J. Z., Zhang, S. X., Yang, S. P., Wang, Z. H., 2020. Development of a validated direct injection-liquid chromatographic tandem mass spectrometric method under negative electrospray ionization for quantitation of nine microcystins and nodularin-R in lake water. J. Chromatogr. A 1609. https://doi:ARTN 46043210.1016/j.chroma.2019.460432

Zhang, Y. Y., Whalen, J. K., Duy, S. V., Munoz, G., Husk, B. R., Sauve, S., 2020b. Improved extraction of multiclass cyanotoxins from soil and sensitive quantification with on-line purification liquid chromatography tandem mass spectrometry. Talanta 216. https://doi:ARTN 12092310.1016/j.talanta.2020.120923

Zheng, N. Y., Taylor, K., Gu, H. D., Santockyte, R., Wang, X. T., McCarty, J., Adelakun, O., Zhang, Y. J., Pillutla, R., Zeng, J. N., 2020. Antipeptide immunocapture with in-sample calibration curve strategy for sensitive and

553 robust LC-MS/MS bioanalysis of clinical protein biomarkers in formalin-fixed paraffin-embedded tumor
554 tissues. Anal. Chem. 92, 14713-14722 https://doi:10.1021/acs.analchem.0c03271

555

Figure Caption：

Fig. 1 Schematic of three different calibration curves approach for the quantitation of microcystins using liquid chromatography tandem mass spectrometry (LC-MS/MS): (A) the traditional multi-sample external calibration curve (MSCC), (B) one sample mulit-point calibration curve (OSCC), and (C) in sample calibration curve (ISCC). And SIL-ISs is adopted in the above three different calibration curves approach.

Fig. 2 The chemical structures of eight microcystins (A) and the multiple isotopologue reaction monitoring (MIRM) chromatograms (B) for each microcystin used for OSCC. In MIRM-OSCC methodology, only the most abundant MIRM channel was used for quantitative analysis for the study samples.

Fig. 3 (A) The MIRM channels of MC-LR observed at three different charge states (singly, doubly, and triply charged ions) under the unit resolution (full width at half height is 0.7 Da) via the triple quadrupole mass spectrometer. Results indicated that the isotopic abundances in MIRM channels with triply charged parent ions is not unacceptable since different MIRM channels would be interference. (B) The response factor ration (mean and standard deviation values) between microcystin and its SIL-IS at the same concentration (1 μg/L) using LC-MS/MS. (C) The measure error values of six different concentration points for microcystins under three calibration curves strategy, including MSCC (a), OSCC (b), and ISCC (c).

Fig. 4 Overview of the validation parameters for eight microcystins under three different calibration curves approach (MSCC, OSCC and ISCC) in spiked blank lake water samples. The recovery and precision (coefficients of variation, CV, %) of eight microcystins under three different calibration curves approach at low, medium and high concentration levels (0.1, 0.3 and 1.0 μg/L for MC-LR, MC-RR, MC-YR, and MC-WR; and 1, 3 and 10 μg/L for MC-LA, MC-LY, MC-LW, and MC-LF) are shown in A and D, B and E, and C and F, respectively.

580 **Table 1** Summary of MIRM parameters for eight microcystins and their SIL-ISs by LC-MS/MS.

Analytes	Element composition of precursor	Retention time (min)	Precursor ion (*m/z*)	Product ion (*m/z*)	Dwell time (ms)	Collision energy (eV)	Relative abundance (%)	Prod ion annotation
MC-LR	$C_{49}H_{76}N_{10}O_{12}$	3.82	498.3	861.5 [a]	20	8	-	$C_{40}H_{65}N_{10}O_{11}^+$
	$[M+2H]^{2+}$		498.3	**135.1** [b]	20	11	100	$C_9H_{11}O^+$
			498.8	135.1	20	11	48.11	-
			499.3	135.1	20	11	13.54	-
			499.3	136.1	20	11	4.76	-
			499.8	136.1	20	11	1.34	-
			499.3	137.1	20	11	0.64	-
MC-LR*	$C_{49}H_{76}{}^{[15]}N_{10}O_{12}$	3.80	503.3	135.1	20	11	-	$C_9H_{11}O^+$
MC-RR	$C_{49}H_{77}N_{13}O_{12}$	2.24	519.8	127.0 [a]	20	49	-	$C_{10}H_7^+$
	$[M+2H]^{2+}$		519.8	**135.1** [b]	20	29	100	$C_9H_{11}O^+$
			520.3	135.1	20	29	49.23	-
			521.3	135.1	20	29	14.70	-
			521.3	136.1	20	29	4.87	-
			521.8	136.1	20	29	1.45	-
			521.3	137.1	20	29	0.64	-
MC-RR*	$C_{49}H_{77}{}^{[15]}N_{13}O_{12}$	2.22	526.3	135.1	20	29	-	$C_9H_{11}O^+$
MC-YR	$C_{52}H_{74}N_{10}O_{13}$	3.64	523.3	911.4 [a]	20	7	-	$C_{41}H_{63}N_{10}O_{12}^+$
	$[M+2H]^{2+}$		523.3	**135.1** [b]	20	10	100	$C_9H_{11}O^+$
			523.8	135.1	20	10	51.37	-
			524.3	135.1	20	10	15.35	-
			524.3	136.1	20	10	5.08	-
			524.8	136.1	20	10	1.52	-
			524.3	137.1	20	10	0.64	-
MC-YR*	$C_{52}H_{74}{}^{[15]}N_{10}O_{13}$	3.65	528.3	135.1	20	10	-	$C_9H_{11}O^+$
MC-WR	$C_{54}H_{75}N_{11}O_{12}$	4.48	534.8	934.5 [a]	20	10	-	$C_{43}H_{64}N_{11}O_{11}^+$
	$[M+2H]^{2+}$		534.8	**135.1** [b]	20	10	100	$C_9H_{11}O^+$
			535.3	135.1	20	10	53.87	-
			535.8	135.1	20	10	16.45	-
			535.8	136.1	20	10	5.33	-
			536.3	136.1	20	10	1.63	-
			535.8	137.1	20	10	0.64	-
MC-WR*	$C_{54}H_{75}{}^{[15]}N_{11}O_{12}$	4.45	540.3	135.1	20	10	-	$C_9H_{11}O^+$
MC-LA	$C_{46}H_{68}N_7O_{12}$	5.53	910.5	213.1 [a]	20	50	-	$C_{14}H_{19}O^+$
	$[M+H]^+$		910.5	**135.1** [b]	20	69	100	$C_9H_{11}O^+$
			911.5	135.1	20	69	43.69	-
			912.5	135.1	20	69	11.54	-
			912.5	136.1	20	69	4.32	-
			913.5	136.1	20	69	1.14	-
			912.5	137.1	20	69	0.64	-
MC-LA*	$C_{46}H_{68}{}^{[15]}N_7O_{12}$	5.52	917.5	135.1	20	69	-	$C_9H_{11}O^+$
MC-LY	$C_{52}H_{72}N_7O_{13}$	5.62	1002.5	163.1 [a]	20	50	-	$C_{11}H_{15}O^+$
	$[M+H]^+$		1002.5	**135.1** [b]	20	73	100	$C_9H_{11}O^+$
			1003.5	135.1	20	73	50.26	-
			1004.5	135.1	20	73	14.77	-
			1004.5	136.1	20	73	4.97	-
			1005.5	136.1	20	73	1.46	-
			1004.5	137.1	20	73	0.64	-
MC-LY*	$C_{52}H_{72}{}^{[15]}N_7O_{13}$	5.60	1009.5	135.1	20	73	-	$C_9H_{11}O^+$
MC-LW	$C_{54}H_{73}N_8O_{12}$	5.92	1025.5	213.1 [a]	20	56	-	$C_{14}H_{19}O^+$
	$[M+H]^+$		1025.5	**135.1** [b]	20	71	100	$C_9H_{11}O^+$
			1026.5	135.1	20	71	52.75	-
			1027.5	135.1	20	71	15.83	-
			1027.5	136.1	20	71	5.22	-
			1028.5	136.1	20	71	1.57	-
			1027.5	137.1	20	71	0.64	-
MC-LW*	$C_{54}H_{73}{}^{[15]}N_8O_{12}$	5.93	1033.5	135.1	20	71	-	$C_9H_{11}O^+$
MC-LF	$C_{52}H_{72}N_7O_{12}$	6.05	986.5	852.5	20	55	-	$C_{43}H_{62}N_7O_{11}^+$
	$[M+H]^+$		986.5	135.1 [a]	20	70	100	$C_9H_{11}O^+$
			987.5	**135.1** [b]	20	70	50.22	-
			988.5	135.1	20	70	14.54	-
			988.5	136.1	20	70	4.97	-
			989.5	136.1	20	70	1.44	-
			988.5	137.1	20	70	0.64	-
MC-LF*	$C_{52}H_{72}{}^{[15]}N_7O_{12}$	6.03	993.5	135.1 [a]	20	70	-	$C_9H_{11}O^+$

581 **Note:** a, this product ion is used as the qualifier ion for each microcystin. b, this is the most abundant ion, which is
582 selected as quantifier ion. The fragment ions of m/z 135.1 and its isotopic ions are used for the preparation of
583 OSCC. To reduce cycle time, dynamic MRM mode was adopted in LC-MS/MS run, and the detection time window
584 was set at 1 min. As for the MRM and MIRM parameters of eight microcystins for MSCC and ISCC are available
585 in Table S1 and Table S2 (supplementary materials), respectively.

Table 2 The element composition and isotopic distributions of neutral loss and daughter ion for eight microcystins and their stable isotopically labeled forms.

Shift	Neutral loss (lost in collision cell)																Shift	Daughter ion	
	MC-LR		MC-RR		MC-YR		MC-WR		MC-LA		MC-LY		MC-LW		MC-LF				
	$C_{40}H_{64}N_{10}O_{11}$		$C_{40}H_{65}N_{13}O_{11}$		$C_{43}H_{62}N_{10}O_{12}$		$C_{45}H_{63}N_{11}O_{11}$		$C_{37}H_{57}N_7O_{11}$		$C_{43}H_{61}N_7O_{12}$		$C_{45}H_{62}N_8O_{11}$		$C_{43}H_{61}N_7O_{11}$			$C_9H_{11}O$	
	m/z	%	*m/z*	%	*m/z*	%	*m/z*	%	*m/z*	%	*m/z*	%	*m/z*	%	*m/z*	%		*m/z*	%
0	860.5	100	903.5	100	910.5	100	933.5	100	775.4	100	867.4	100	890.4	100	851.4	100	0	135.1	100
1	861.5	48.11	904.5	49.23	911.5	51.37	934.5	53.87	776.4	43.69	868.4	50.26	891.4	52.75	852.4	50.22	1	136.1	9.9
2	862.5	13.54	905.5	14.70	912.5	15.35	935.5	16.45	777.4	11.54	869.4	14.77	892.4	15.83	853.4	14.54	2	137.1	0.64
3	863.5	2.76	906.5	2.85	913.5	3.32	936.5	3.59	778.4	2.22	870.4	3.16	893.4	3.44	854.4	3.05	3	138.1	0.03
	MC-LR		MC-RR		MC-YR		MC-WR		MC-LA		MC-LY		MC-LW		MC-LF				
	$C_{40}H_{64}{}^{[15]}N_{10}O_{11}$		$C_{40}H_{65}{}^{[15]}N_{13}O_{11}$		$C_{43}H_{62}{}^{[15]}N_{10}O_{12}$		$C_{45}H_{63}{}^{[15]}N_{11}O_{11}$		$C_{37}H_{57}{}^{[15]}N_7O_{11}$		$C_{43}H_{61}{}^{[15]}N_7O_{12}$		$C_{45}H_{62}{}^{[15]}N_8O_{11}$		$C_{43}H_{61}{}^{[15]}N_7O_{11}$			$C_9H_{11}O$	
	m/z	%	*m/z*	%	*m/z*	%	*m/z*	%	*m/z*	%	*m/z*	%	*m/z*	%	*m/z*	%		*m/z*	%
0	870.5	100	916.5	100	920.5	100	944.5	100	782.4	100	874.4	100	898.4	100	858.4	100	0	135.1	100
1	871.5	44.42	917.5	44.43	921.5	47.68	945.5	49.81	783.4	41.1	875.4	47.67	899.4	49.8	859.4	47.63	1	136.1	9.9
2	872.5	11.88	918.5	11.88	922.5	13.57	946.5	14.39	784.4	10.48	876.4	13.57	900.4	14.39	860.4	13.34	2	137.1	0.64
3	873.5	2.36	919.5	2.36	923.5	2.86	947.5	3.05	785.4	1.98	877.4	2.85	901.4	3.05	861.4	2.74	3	138.1	0.03

Note: The shift means the mass shift for neutral loss or daughter ion. The isotopic abundance of MIRM channel = (relative isotopic distribution of the neutral loss)×(relative isotopic distribution of the corresponding daughter ion), in which the mass shift value of daughter ion should be higher or equal to that neutral loss. The element composition for the daughter ion and neutral loss for eight microcystins is obtained by LC-HRMS (Q/Orbitrap-MS), and the detail information about accurate MS/MS spectra for eight microcystins is available in supplementary materials Fig. S1.

592 **Table 3** Summary of the linearity range, correlation coefficient, LOD and LOQ for eight
593 microcystins using LC-MS/MS under three different calibration curves.

Analytes	Multi-sample external calibration curve (MSCC)				One sample external calibration curve (OSCC)				In sample calibration curve (ISCC)			
	Linearity range (µg/L)	r2	LOD (µg/L)	LOQ (µg/L)	Linearity range (µg/L)	r2	LOD (µg/L)	LOQ (µg/L)	Linearity range (µg/L)	r2	LOD (µg/L)	LOQ (µg/L)
MC-LR	0.05-10.0	0.987	0.02	0.05	0.064-10.0	0.997	0.02	0.064	0.064-10.0	0.998	0.020	0.064
MC-RR	0.05-10.0	0.992	0.02	0.05	0.064-10.0	0.997	0.02	0.064	0.064-10.0	0.999	0.020	0.064
MC-YR	0.05-10.0	0.994	0.02	0.05	0.064-10.0	0.998	0.02	0.064	0.064-10.0	0.999	0.020	0.064
MC-WR	0.05-10.0	0.991	0.02	0.05	0.064-10.0	0.997	0.02	0.064	0.064-10.0	0.999	0.020	0.064
MC-LA	0.50-100.0	0.984	0.20	0.50	0.64-100.0	0.999	0.20	0.64	0.64-100.0	0.999	0.20	0.64
MC-LY	0.50-100.0	0.982	0.20	0.50	0.64-100.0	0.999	0.20	0.64	0.64-100.0	0.999	0.20	0.64
MC-LW	0.50-100.0	0.993	0.20	0.50	0.64-100.0	0.998	0.20	0.64	0.64-100.0	0.999	0.20	0.64
MC-LF	0.50-100.0	0.987	0.20	0.50	0.64-100.0	0.998	0.20	0.64	0.64-100.0	0.999	0.20	0.64

594 **Note**: A least-squares linear regression without weight is used for three different calibration curves, including
595 MSCC, OSCC and ISCC. In the traditional MSCC, the LODs and LOQs for each microcystin are assessed
596 according to the S/N >3 and 10, respectively, while in OSCC and ISCC the LOQs is originated from the less
597 abundant MIRM channel.

598 **Table 4** Concentrations of eight microcystins in different lake water samples collected in China
599 during autumn seasons.

Location	No.	MC-LR (μg/L)	MC-RR (μg/L)	MC-YR (μg/L)	MC-WR (μg/L)	MC-LA (μg/L)	MC-LY (μg/L)	MC-LW (μg/L)	MC-LF (μg/L)
	1	<LOQ	0.24	0.15	ND	ND	ND	ND	ND
	2	0.16	ND	ND	ND	ND	ND	ND	ND
	3	0.15	0.09	ND	ND	ND	ND	ND	ND
	4	ND	0.08	ND	ND	ND	ND	ND	ND
Lake Tai	5	0.38	1.32	0.87	ND	ND	<LOQ	ND	ND
(Suzhou)	6	ND	ND	ND	ND	ND	ND	ND	ND
	7	0.37	0.13	<LOQ	ND	ND	<LOQ	ND	ND
	8	<LOQ	ND	ND	ND	ND	ND	ND	ND
	9	0.18	ND	ND	<LOQ	ND	ND	ND	ND
	10	0.83	0.45	0.22	ND	ND	ND	<LOQ	ND
	11	2.80	3.90	0.96	<LOQ	ND	ND	ND	ND
	12	0.35	0.18	ND	ND	ND	ND	ND	ND
	13	0.09	ND	ND	ND	ND	ND	ND	ND
	14	ND	0.31	ND	ND	ND	ND	ND	ND
Chaohu Lake	15	ND	ND	0.16	ND	ND	ND	ND	ND
(Chaohu)	16	0.86	1.84	2.27	ND	ND	ND	<LOQ	ND
	17	2.69	12.40	3.62	<LOQ	0.96	<LOQ	1.24	ND
	18	ND	ND	ND	ND	ND	ND	ND	ND
	19	0.45	0.43	0.16	ND	ND	ND	ND	ND
	20	ND	0.12	ND	ND	ND	ND	ND	ND

600 Note: The concentration for each microcystin was obtained by MIRM-LC-MS/MS via OSCC methodology.
601 Additionally, in comparison with the traditional MSCC and ISCC methodology, the measured values is almost the
602 same, in which the errors is less than 8.7%.
603

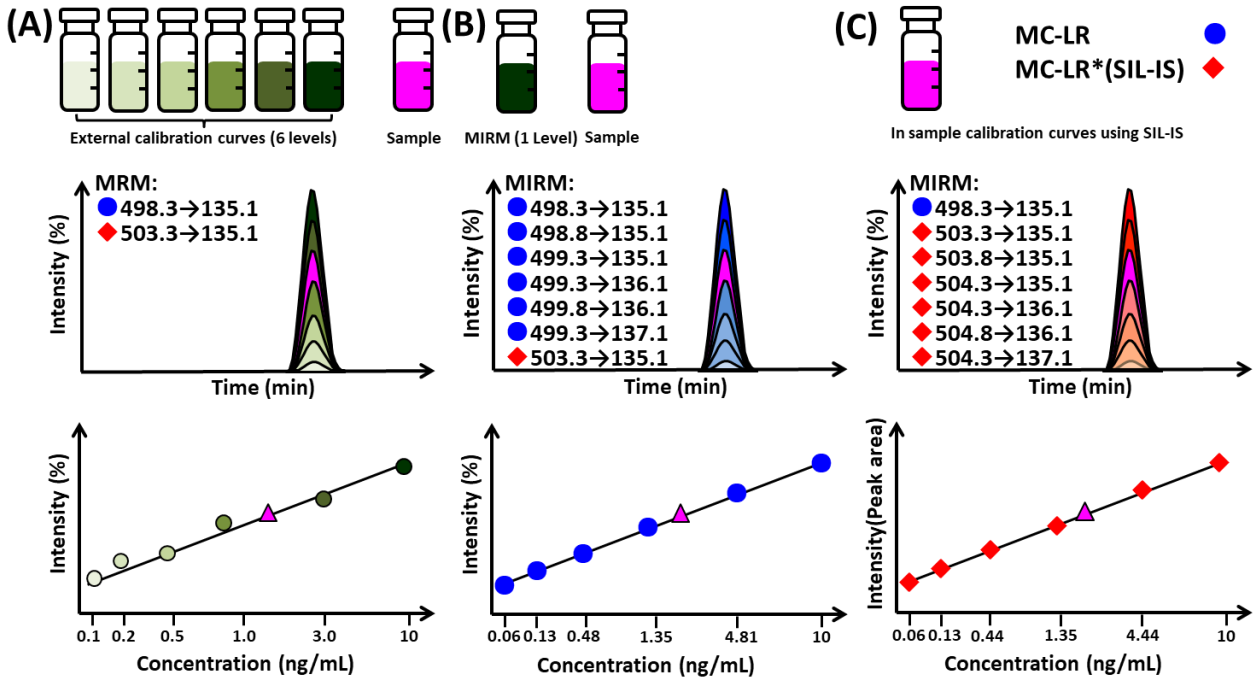
(A)
External calibration curves (6 levels)
Sample
(B)
MIRM (1 Level)
Sample
(C)
MC-LR
MC-LR*(SIL-IS)
In sample calibration curves using SIL-IS
MRM:
498.3→135.1
503.3→135.1
Intensity (%)
Time (min)
MIRM:
498.3→135.1
498.8→135.1
499.3→135.1
499.3→136.1
499.8→136.1
499.3→137.1
503.3→135.1
Intensity (%)
Time (min)
MIRM:
498.3→135.1
503.3→135.1
503.8→135.1
504.3→135.1
504.3→136.1
504.8→136.1
504.3→137.1
Intensity (%)
Time (min)
Intensity (%)
0.1 0.2 0.5 1.0 3.0 10
Concentration (ng/mL)
Intensity (%)
0.06 0.13 0.48 1.35 4.81 10
Concentration (ng/mL)
Intensity(Peak area)
0.06 0.13 0.44 1.35 4.44 10
Concentration (ng/mL)

Fig. 1

608

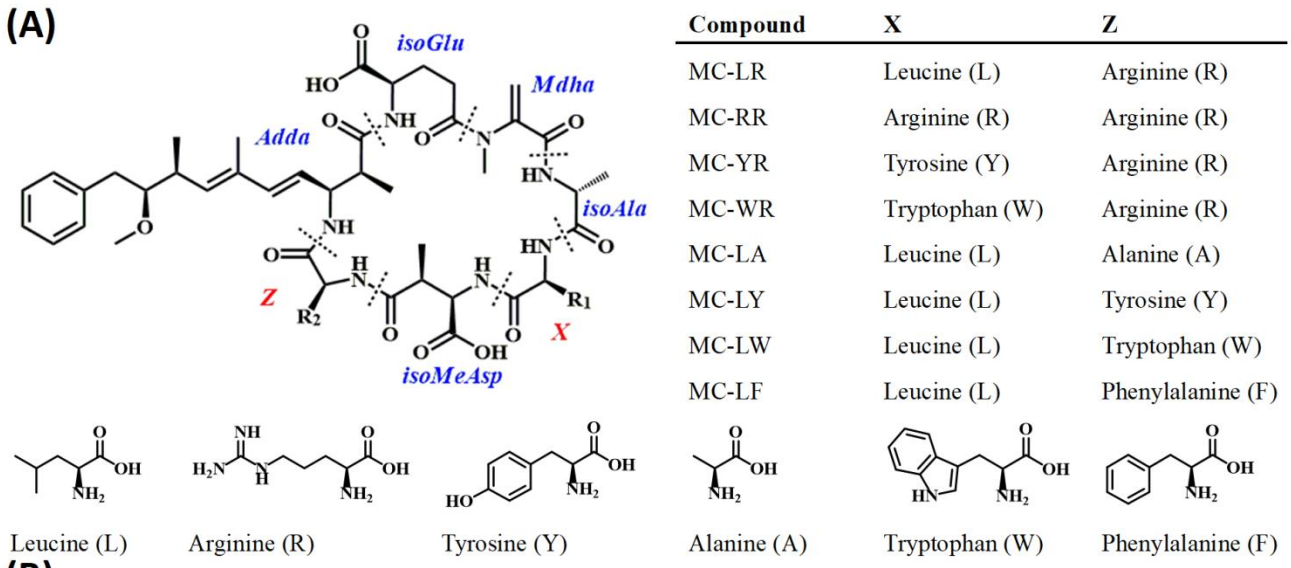

Compound	X	Z
MC-LR	Leucine (L)	Arginine (R)
MC-RR	Arginine (R)	Arginine (R)
MC-YR	Tyrosine (Y)	Arginine (R)
MC-WR	Tryptophan (W)	Arginine (R)
MC-LA	Leucine (L)	Alanine (A)
MC-LY	Leucine (L)	Tyrosine (Y)
MC-LW	Leucine (L)	Tryptophan (W)
MC-LF	Leucine (L)	Phenylalanine (F)

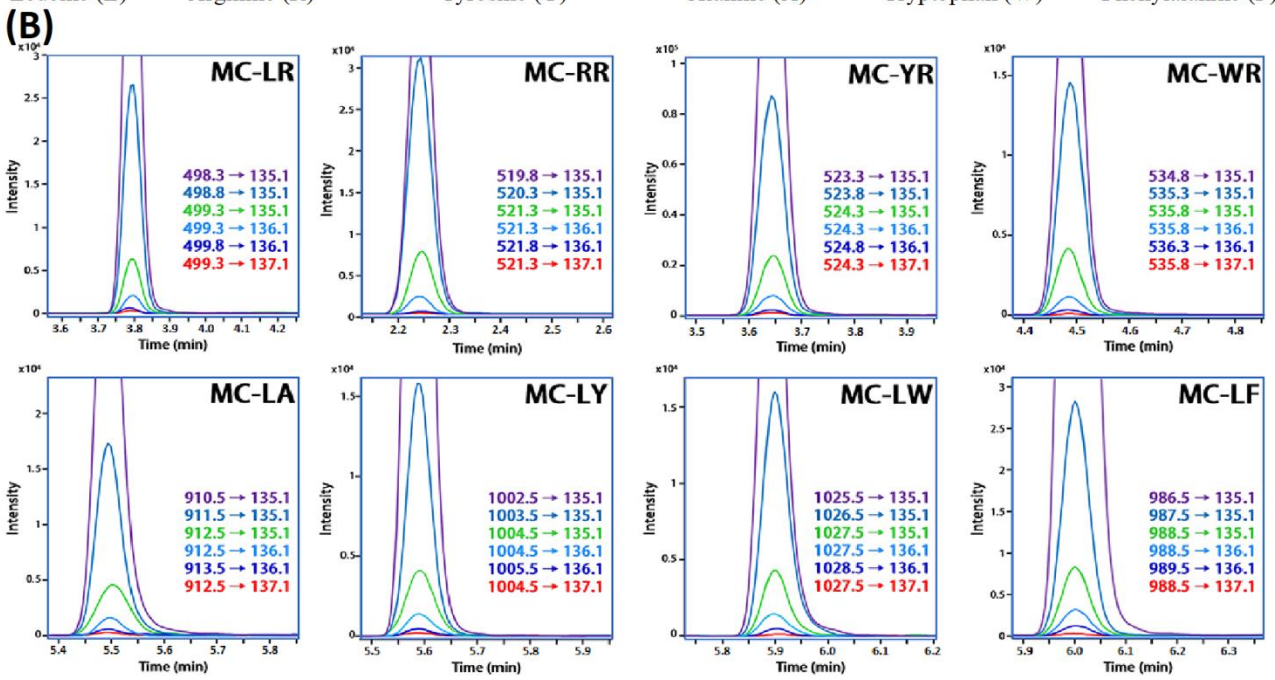

609

610 **Fig. 2**

611

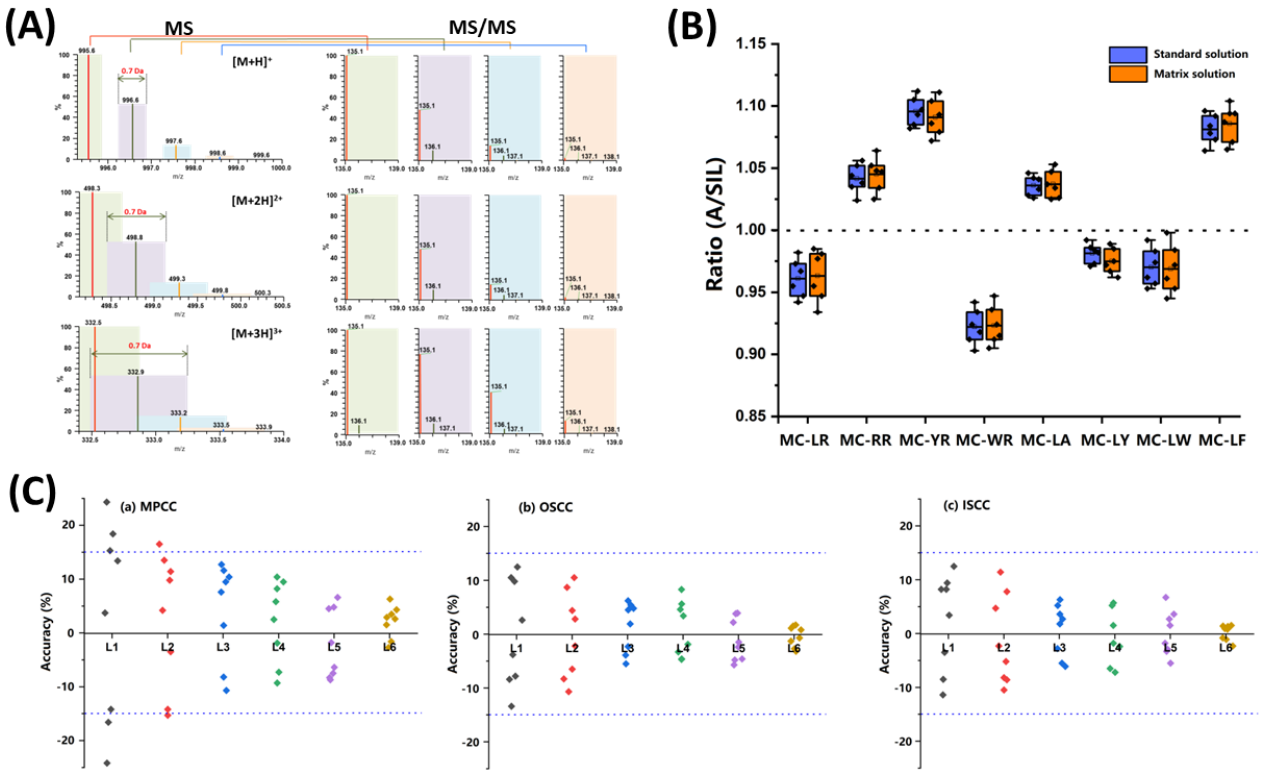
(A)
MS
MS/MS
[M+H]+
[M+2H]2+
[M+3H]3+
0.7 Da
(B)
Standard solution
Matrix solution
Ratio (A/SIL)
MC-LR
MC-RR
MC-YR
MC-WR
MC-LA
MC-LY
MC-LW
MC-LF
(C)
(a) MPCC
(b) OSCC
(c) ISCC
Accuracy (%)
L1
L2
L3
L4
L5
L6

Fig. 3

616

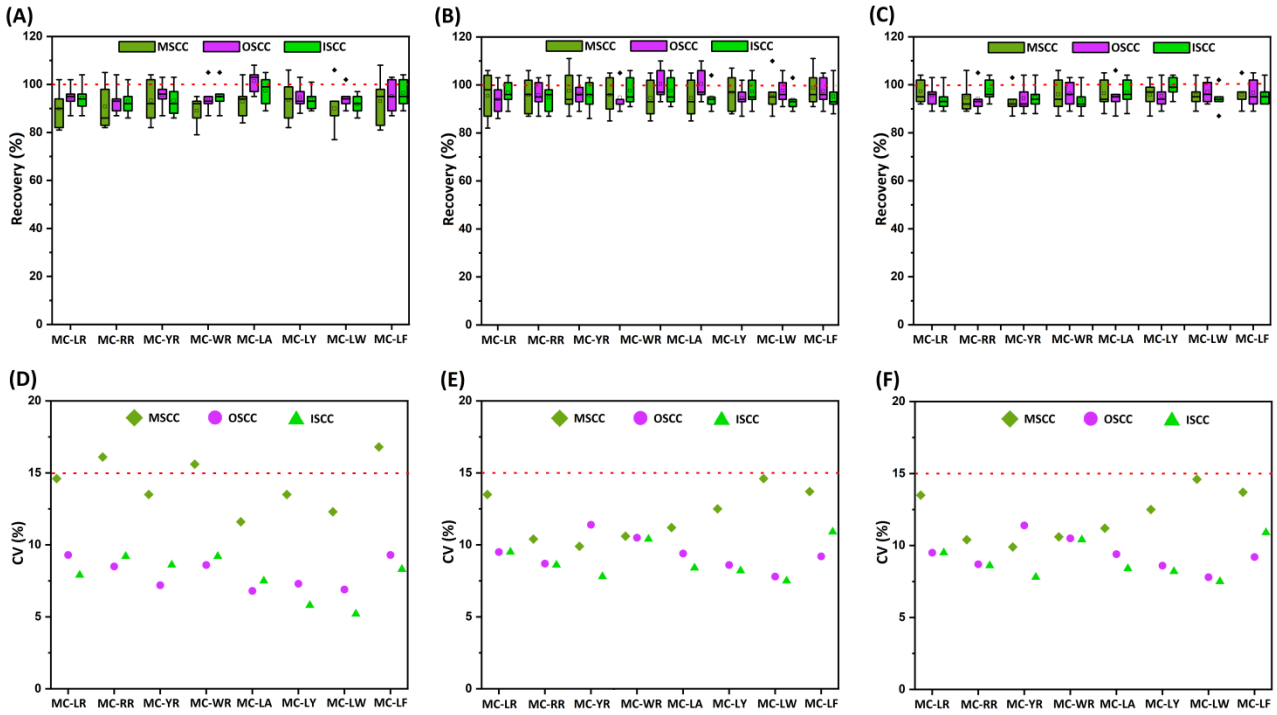

617

618 **Fig. 4**

Declaration of interests

☒The authors declare that they have no known competing financial interests or personal relationships that could have appeared to influence the work reported in this paper.

☐The authors declare the following financial interests/personal relationships which may be considered as potential competing interests:

CRediT authorship contribution statement

Huiyan Zhang: Conceptualization, data curation, methodology and writing the original draft. **Yanshen Li**: data curation, and methodology. **Mohamed F. Abdallah**: writing and revising the draft. **Jianxun Li, Shuyan Liu, and Rong Zhang**: methodology and revising the draft. **Feifei Sun**: writing and revising the draft. **Yi, Li:** Supervision. **Shupeng Yang**: Supervision, conceptualization and funding acquisition.